8th International Symposium on Magnetic Bearing
August 26-28, 2002, Mito, Japan

CONTROLLER DESIGN FOR A MAGNETICALLY SUSPENDED MILLING SPINDLE BASED ON CHATTER STABILITY ANALYSIS

Jin-Ho Kyung
Intelligence and Precision Machine Department,
Korea Institute of Machinery and Materials, P.O.Box 101, Yusung, Daejeon 305-600, Korea,
jhkyung@kimm.re.kr

Chong-Won Lee
Center for Noise and Vibration Control, KAIST, Science Town, Daejeon 305-701, Korea,
cwlee@novic.kaist.ac.kr

ABSTRACT

The chatter stability of a rigid milling spindle levitated by five-axes active magnetic bearings (AMBs) is studied for its chatter free cutting, as the control gains of AMBs vary. The characteristic equation for regenerative chatter loop with a delay element is described by a linear differential-difference equation, accounting for the dynamics of the AMB controllers, the uncut chip thickness equation and the cutting process as well as the rigid spindle dynamics itself. An efficient chatter stability analysis method is then proposed to predict the stability lobes and chatter frequency in milling. The analytically predicted stability lobes are found to be in good agreement with the lobes generated by other methods available in the literature. Using the proposed method, parametric study is also performed to investigate the influences of the damping and stiffness coefficients of AMBs on the chatter free cutting conditions, as they are allowed to vary within the stable region formed by the AMB control gains.

INTRODUCTION

Modern high speed machine tool spindles are often equipped with active magnetic bearings (AMBs), because of such advantages as free of friction loss and maintenance, and process monitoring capability during operation. High speed cutting using the spindle levitated by AMBs offers high material removal rates, high surface quality accompanied by high shape and form accuracy, reduced burr formation, less damage of surface integrity, possibility of machining of thin webs and higher stability in cutting due to less vibration [1].

Machine tool chatter is a self-excited vibration that is mainly caused by the interaction between a machine tool-workpiece structure and cutting process dynamics, and it is indeed one of the major constraints that limit productivity of machining process. Chatter leads to poor surface finish and dimensional accuracy in a machined part, fast wear and breakage of a cutting tool, and even severe damage to a machine tool. In order to develop chatter-free cutting conditions for a high speed machine tool spindle, the stability analysis for machine tool chatter and the efficient analysis method need to be developed [1,2].

Many rigorous methods have been developed to predict the onset of chatter. Tlusty and Polacek [3] presented a practical stability law for orthogonal cutting systems. Merritt [4] assumed no dynamics in the cutting process and developed a theory to calculate the stability boundary by plotting a gain-phase of the harmonic response functions of the cutting process and the structure on the critical loci plot. The first comprehensive theoretical analysis of milling stability has been performed by Sridhar, et al.[5]. Lee and Liu [6] utilized the Nyquist criterion to numerically calculate the stability limits. Altintas and Budak [7] presented an analytical method to solve the eigenvalue problem associated with the chatter stability for end milling operations. But, an iteration procedure was required to search for the chatter frequencies associated with all dominant structural modes. However, cumbersome numerical manipulations are involved in most conventional methods.

In order to overcome such numerical difficulties encountered in the conventional methods, development of an analysis method is required to efficiently formulate the structural dynamics coupled with cutting process. For the milling spindle with AMBs, the effects of the AMB controller dynamics on chatter stability need to be investigated. The optimum AMB's control gains for chatter-free cutting should then be determined based on the analysis results. So far, a few works are available, which deal with the chatter analysis of a milling spindle with AMBs. However, their contributions were restricted to experimental evaluation of the cutting performance and tool wear of a high speed spindle with AMBs [2].

This work focuses on the AMB controller design based on the stability analysis for regenerative chatter in a milling spindle. The characteristic equation for regenerative chatter loop with a delay element is described by a linear differential-difference equation, accounting for the dynamics of the AMB controllers, the

uncut chip thickness equation and the cutting process as well as the rigid spindle dynamics itself. An efficient chatter stability analysis method using Pade approximant [8] for the delay element is then proposed to predict the stability lobes and chatter frequency. Using the proposed method, parametric study is also performed to investigate the influences of the damping and stiffness coefficients of AMBs on the chatter free cutting conditions, as they are allowed to vary within the stable region formed by the AMB control gains. Finally, the effective adjustment of stiffness and damping of AMB for chatter-free cutting in milling is discussed.

THE GENERAL OF CHARACTERISTIC EQUATION FOR REGENERATIVE CHATTER

Uncut Chip-Thickness Equation

Regenerative chatter occurs due to undulations on an earlier cut surface by a previous cutter [9]. In order to derive a feedback loop representing the chatter, the cutting process will be illustrated in a milling spindle with AMBs as shown in Figures 1 and 2. A milling cutter can be considered to have two orthogonal degrees of freedom as shown in Figure 2. The spindle with a N flute end mill cutter is levitated by five-axes magnetic bearings. The feed rate is adjusted to obtain an average or steady state depth of cut. The uncut chip-thickness equation for milling process can be described as

$$U = (U_o + S_{j-1} - S_j)\, g(\varphi_j) \tag{1}$$

where $g(\phi_j) = \begin{cases} 1 & \text{for } \phi_{st} < \phi_j < \phi_{ex} \\ 0 & otherwise \end{cases}$,

$$U = \{u_Y(t), u_Z(t)\}^T,\ U_o = \{u_{oY}, u_{oZ}\}^T$$

$$S_{j-1} = \frac{1}{\mu}\left\{Y_c(t-\frac{T}{N}), Z_c(t-\frac{T}{N})\right\}^T,\ S_j = \{Y_c, Z_c\}^T$$

Here $Y_c(t), Z_c(t)$ are the displacements of the cutter in the Y, Z directions; T/N is the delay time; u_Y, u_Z are the Y, Z directional components of the uncut chip thickness;

u_{oY}, u_{oZ} ($u_{oY} = u_{oZ} = \frac{u_o}{(\phi_{ex} - \phi_{st})}(\cos\phi_{st} - \cos\phi_{ex})$) are the Y, Z directional components of the feed rate; N, μ, T, ϕ_{st} and ϕ_{ex} are the number of tooth, the overlap factor (μ =1 for the worst case), the tooth period, and, the start and exit immersion angles of the cutter to the cut, respectively.

Cutting Process Equation

The resultant cutting force, $f(t)$, is related to the displacements of the cutter, U. The cutting process dynamics is normally neglected, and the directional dynamic milling force coefficients are often approximated to be time-invariant but immersion dependent, only taking the average component of their Fourier series expansion. Following the procedure proposed in Altintas and Budak [7], the cutting process can be expressed as:

$$f = \tfrac{1}{2} b K_t A_o U \tag{2}$$

where $f = \{F_Y \ \ F_Z\}^T$, $A_o = \begin{bmatrix} A_{oYY} & A_{oYZ} \\ A_{oZY} & A_{oZZ} \end{bmatrix}$

$$A_{oYY} = \frac{1}{2(\phi_{exj} - \phi_{stj})}\left[-\cos 2\phi_j - 2K_r\phi_j - K_r \sin 2\phi_j\right]_{\phi_{stj}}^{\phi_{exj}}$$

$$A_{oYZ} = \frac{1}{2(\phi_{exj} - \phi_{stj})}\left[-\sin 2\phi_j + 2\phi_j + K_r \cos 2\phi_j\right]_{\phi_{stj}}^{\phi_{exj}}$$

$$A_{oZZ} = \frac{1}{2(\phi_{exj} - \phi_{stj})}\left[\cos 2\phi_j - 2K_r\phi_j + K_r \sin 2\phi_j\right]_{\phi_{stj}}^{\phi_{exj}}$$

$$A_{oZY} = \frac{1}{2(\phi_{exj} - \phi_{stj})}\left[-\sin 2\phi_j - 2\phi_j + K_r \cos 2\phi_j\right]_{\phi_{stj}}^{\phi_{exj}}$$

Here K_t and K_r are the tangential and radial cutting coefficients; b is the axial depth of cut; F_Y and F_Z are the cutting forces in the Y and Z directions. Since the average cutting force per tooth period is independent of the helix angle of helical end mills, the above expression for A_o is valid for them as well.

Dynamic Equation of Rigid Milling Spindle With AMBs

Assuming, without loss of generality, that the axial and radial spindle motions are not coupled each other so that the axial AMB control is independent of the radial AMBs control, we can write the governing equation of motion associated with the radial motion of the spindle as

$$\boldsymbol{M_c}\,\ddot{\boldsymbol{q}}_s + \boldsymbol{G_c}\,\dot{\boldsymbol{q}}_s + \boldsymbol{K_{cy}}\,\boldsymbol{q}_s = \boldsymbol{B_c}\,\boldsymbol{i} + \boldsymbol{B_F}\,\boldsymbol{f}$$

$$\boldsymbol{i} = -\boldsymbol{K_{amp}}\boldsymbol{K_p}\boldsymbol{K_s}\boldsymbol{q_s} - \boldsymbol{K_{amp}}\,\boldsymbol{K_d}\boldsymbol{K_s}\,\dot{\boldsymbol{q}}_s \tag{3}$$

where $\boldsymbol{q_s} = \{y_1, y_2, z_1, z_2\}^T$, $\boldsymbol{i} = \{i_{y1}, i_{y2}, i_{z1}, i_{z2}\}^T$

Here $\boldsymbol{M_c}$, $\boldsymbol{G_c}$, $\boldsymbol{K_{cy}}$, $\boldsymbol{B_F}$, $\boldsymbol{B_c}$, $\boldsymbol{K_p}$ and $\boldsymbol{K_d}$ denote the mass, gyroscopic, stiffness, coordinate transform, current stiffness, proportional and derivative gain matrices, respectively, and the detailed expressions are given in Appendix A; $\boldsymbol{q_s}$ and $\boldsymbol{i}$ are the displacement and control current vectors at sensor positions; m, I_p and I_t are the mass, diametrical and polar mass moments of inertia of rotor; l_{s1} and l_{s2} are the distances of the sensors from the C.G. point of rotor; l_{c1} and l_{c2} are the distances of two radial magnetic bearings from the C.G. point of rotor; l_c is the distance of the milling cutter from the C.G. point of rotor; Ω is the rotational speed; the position and current stiffnesses, $k_{y1}, k_{y2}, k_{z1}, k_{z2}, k_{iy1}, k_{iy2}, k_{iz1}$ and k_{iz2} are defined from the linearized magnetic forces; $\boldsymbol{K_{amp}}$ and

K_s are the constant power amplifier and sensor gain diagonal matrices; $k_{py1}, k_{py2}, k_{pz1}, k_{pz2}, k_{dy1}, k_{dy2}, k_{dz1}$ and k_{dz2} are the proportional and derivative gains.

The gyroscopic effect can be neglected when the polar mass moment of inertia of the spindle is small relative to the diametrical mass moment of inertia of the rotor. AMB can be designed so that the off-diagonal elements of the mass matrix are neglected. The whole AMB system can be reduced to five decoupled single-axis AMB systems, according to their own design specifications. Then the decentralized PD controller can be utilized for each decoupled system

The displacements of the cutter can be expressed as

$$\boldsymbol{S}_j = \boldsymbol{T}_c \boldsymbol{q}_s \tag{4}$$

where

$$\boldsymbol{T}_c = \begin{bmatrix} \frac{L_1+L_2}{L_1} & -\frac{L_2}{L_1} & 0 & 0; & 0 & 0 & \frac{L_1+L_2}{L_1} & -\frac{L_2}{L_1} \end{bmatrix}$$

$L_1 = l_{s1} + l_{s2}$, $L_2 = l_c - l_{s1}$

Substituting Eqs. (1), (2) and (4) into Eq. (3) and rearranging the resulting expression, we obtain

$$M_c \ddot{q}_s + (G_c + B_c K_{amp} K_d K_s)\dot{q}_s +$$

$$\frac{1}{2\mu} b K_i B_F A_0 T_c (q_{s-1} - q_s) + (K_{cy} + B_c K_{amp} K_c K_s) q_s$$

$$= \frac{1}{2} b K_i B_F A_0 U_0 \tag{5}$$

where $q_{s-1} = \left\{ y_1(t-\frac{T}{N}), y_2(t-\frac{T}{N}), z_1(t-\frac{T}{N}), z_2(t-\frac{T}{N}) \right\}^T$

Characteristic Equation

Substituting $q_s = q_{s0} e^{\lambda t}$ into the homogeneous part of equation of motion (5), we get the characteristic equation of the chatter loop given by

$$M_c \lambda^2 + (G_c + B_c K_{amp} K_d K_s)\lambda +$$

$$\frac{1}{2\mu} b K_i B_F A_0 T_c (e^{-\frac{T}{N}\lambda} - 1) + K_{cy} + B_c K_{amp} K_c K_s = 0 \tag{6}$$

which is transcendental due to the delay element, $e^{-\frac{T}{N}\lambda}$. It is clear that the variations in the time delay and the depth of cut significantly affect the stability of the system. Note that the characteristic equation is also dependent upon the gains of the magnetic bearings, which thus affect the chatter stability.

STABILITY ANALYSIS FOR REGENERATIVE CHATTER

Stability of Chatter Loop

The stability lobe diagram is commonly constructed by experiments or theoretical predictions in order to select appropriate cutting parameters for chatter-free cutting. The stability lobe diagram may be plotted for the depth of cut and the spindle speed for each stability lobes. In this section, we propose a new stability analysis method.

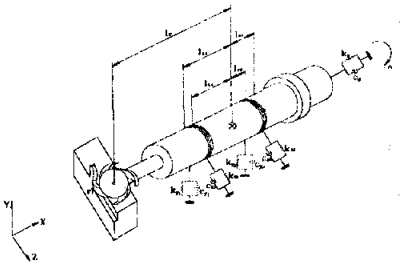

FIGURE 1: Coordinate system of the milling spindle

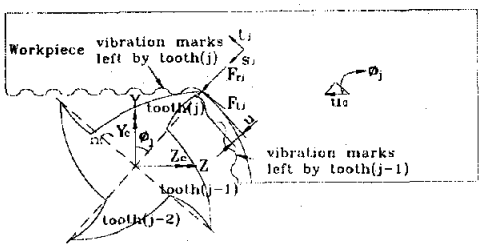

FIGURE 2: Dynamic model of milling process

Regenerative Chatter Analysis

Nonrational Function. The nonrational delay function, $e^{-\frac{T}{N}\lambda}$, in the characteristic equation (6) is approximated as a rational function. It is obtained by the Taylor series expansion of the delay function, that is, by a (p, q) Pade approximant[9], whose numerator and denominator are a polynomial of degree p and q, respectively. For $p = q = 2$, the delay function is well approximated by the (2, 2) Pade approximant, i. e.

$$e^{-\frac{T}{N}\lambda} \cong \frac{\frac{1}{12}\left(\frac{T}{N}\right)^2 \lambda^2 - \frac{1}{2}\left(\frac{T}{N}\right)\lambda + 1}{\frac{1}{12}\left(\frac{T}{N}\right)^2 \lambda^2 + \frac{1}{2}\left(\frac{T}{N}\right)\lambda + 1} \tag{7}$$

Eigenvalue Problem. We now consider an mxn matrix whose elements are polynomials in a scalar λ; the coefficients of the polynomials may be complex numbers. Such a matrix may be considered as a polynomial in λ whose coefficients are constant mxn matrices. If p is the highest power of λ appearing among the elements, the λ-matrix associated with the approximated characteristic equation by substituting the (2, 2) Pade approximant into Eq. (6) becomes, following the procedure described in Lee [10].

$$D_p(\lambda) = E_p \lambda^p + E_{p-1} \lambda^{p-1} + \ldots + E_1 \lambda^1 + E_0 \tag{8}$$

where $\lambda = \sigma + i\omega$, σ and ω being the real and imaginary part of λ, respectively. Here E_i, $i = 0, 1, \ldots, p$, are the mxn matrices with complex elements. The generalized eigenvalue problem from the λ-matrix

is formulated as

$$A\lambda = B \tag{9}$$

The details of A and B are given in Appendix B. The eigenvalue problem (9) can then be easily solved by using a commercial code such as Matlab.

Chatter Frequency. With the time delay, T, varied, we can find the chatter frequency ω_c from Eq. (9) by letting $\sigma = 0$.

Phase Angle. The quantity φ is the predicted phase angle in radians of the regenerative wave on the machined surface at the tool face relative to the wave actually being cut. The phase angle is determined as

$$\cos(T\frac{\omega_c}{N}) - j\sin(T\frac{\omega_c}{N}) \cong \Lambda_R + j\Lambda_I \text{, or,}$$

$$\varphi = T\frac{\omega_c}{N} \cong \tan^{-1}(\frac{-\Lambda_I}{\Lambda_R}) \tag{10}$$

Here Λ_R, Λ_I are the real and imaginary parts of the Pade approximant at a chatter frequency. Equation (10) is derived from approximating the delay function using the Pade approximant at a chatter frequency. The approximated phase angle is effective in the region $[-\pi, \pi]$ with about 10 % or less error.

Stability Lobe Diagram. It is convenient to express the phase angle for the stability lobe diagram as an integer number of cycles, n, plus a fractional portion of a cycle, $\nu = \varphi/(2\pi)$; that is

$$\omega_c\frac{\tilde{T}}{N} = 2\pi(n+\nu) = 2\pi f\frac{\tilde{T}}{N} \tag{11}$$

Since n is an integer, $e^{-j2\pi n} = 1$ and, therefore, $e^{-j2\pi(n+\nu)} = e^{-j2\pi\nu}$.

Here ν is defined as the phase factor and has a range $0 \le \nu \le 1$; $\tilde{T}$ and f are the predicted time delay and the chatter frequency in Hz. Note that if the phase angle $\varphi < 0$ than additional 2π must be added to the phase angle in the calculation of the phase factor.

The stability lobe diagram can be plotted by two methods. The first method uses the relation, for seeking the lobes, given by

$$V = \frac{1}{\tilde{T}} = \frac{f}{N(n+\nu)} \quad \text{from equation (11)} \tag{12}$$

where V is the spindle rotational speed. Using b and V calculated can plot the stability lobe diagram. The second method predicts the unstable region (upper part of the stability lobes) using the Routh-Hurwitz criterion [8] based on ordering the characteristic equation into an array. The second is faster than the first in predicting the lower lobes such as 0-lobe or 1-lobe, but it is restricted to the case of the predicted phase angle bounded by $[-\pi, \pi]$, because the Pade approximant is only effective in the region with less than 10 % error. These methods can be applied to other machining processes, as long as the system equations are expressed as a set of linear time invariant difference-differential equations.

Example. A single degree of freedom model [4] is considered to compare the proposed stability analysis method with other methods. Figure 3 compares the stability lobes obtained by three different methods, where the solid line, the marks 'o' and '+' represent the results by the Merritt [4], Altintas and Budak [7] and proposed methods, respectively. The analytically predicted stability lobes by the proposed method are found to be in good agreement with other commonly used methods.

MILLING SPINDLE MODEL WITH AMBS

The milling spindle system with AMBs is shown in Figure 4, which consists of two hetero-polar radial magnetic bearings, an axial magnetic bearing, a milling cutter and a driving motor (5.5 kW). Some important dimensions and specifications of the system are as follows:

- Spindle : length(280 mm), average diameter(49.2 mm), total weight with one flute cemented carbide milling cutter(4.37 kg)
- AMB : air gap(0.4 mm), areas of pole(300 mm^2 for front bearing, 200 mm^2 for rear bearing), number of turn(110 per leg), bias currents in the radial bearings(3 A), amplifier time constant (0.0001 sec), low pass filter time constant of the PD controller(0.000032 sec)

THEORETICAL RESULTS

To investigate the influence of the proportional and derivative gains on chatter stability, the critical axial depth of cuts were calculated by using the proposed method, as the gains were varied within the stable region of the AMBs. The stable regions of the AMBs were experimentally determined as:

1) Front AMB : Proportional gain (k_p) ; 0.9 – 4.5, derivative gain (k_d) ; 0.0003- 0.0053
2) Rear AMB : Proportional gain (k_p) ; 1 – 7 , derivative gain (k_d) ; 0.0002- 0.01

The cutting coefficient for aluminum alloy workpiece used for stability analysis was taken as 1,500,000,000 N/m [7,11]. In the analysis, the start and exit immersion angles were kept to be 0 and 90 degrees, respectively. In the simulations, the gains were varied ranging from about + 35 % to – 35 % of the reference gains of the AMBs. The reference gains are:

1) Front proportional gain: 1.6, front derivative gain: 0.0016
2) Rear proportional gain: 1.6, rear derivative gain: 0.0032

Successive simulation was taken with increasing the axial depth of cut up to 2 mm, until the stability lobes(5 lobes) with the chatter frequency is encountered.

Figure 5 and 6 show the stability lobes with the

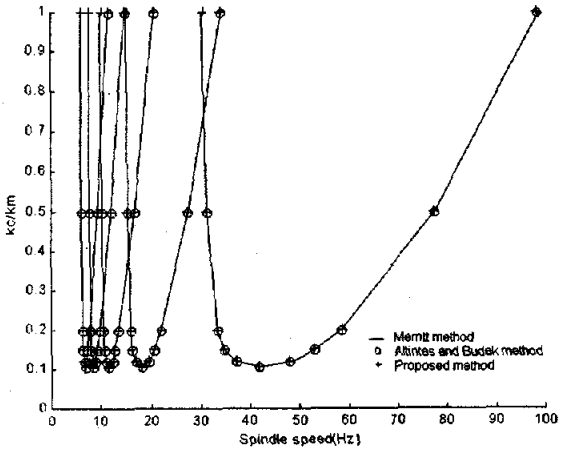

FIGURE 3: Comparison of predicted chatter limits

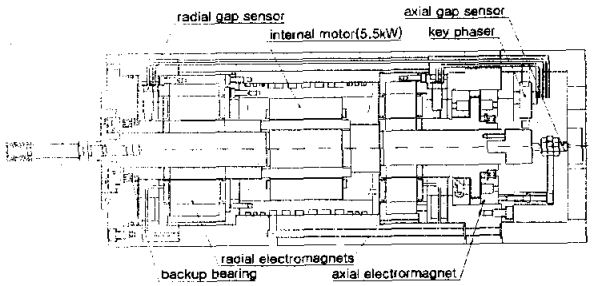

FIGURE 4: Schematic diagram of the milling spindle with AMBs

proportional and derivative gains in the front AMB varied when the proportional and derivative gains of the rear AMB are fixed at k_p = 1.6 and k_d = 0.002. Figure 5 indicates that the stable region increases as the proportional gain increases over the speed range lower than about 6,000 rpm. But, the predicted lobes indicate the higher stability over the speed range higher than about 6,000 rpm, as the proportional gain decreases. When the front AMB derivative gain is large, the stable region is likely to be increased over the whole speed range, as shown in Figure 6. For these reasons, the small proportional and large derivative gains for the front AMB are recommended in high speed cutting.

Figures 7 and 8 show the stability lobes with the proportional and derivative gains of the rear AMB varied when the proportional and derivative gains of the front AMB are fixed at k_p = 1.6 and k_d = 0.0016. Note that, unlike the front AMB, the stable regions were not sensitive to the proportional and derivative gains of the rear bearing.

SUMMARY

The accomplishments of this work can be summarized as follows.

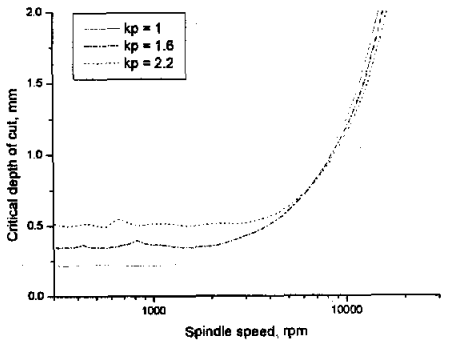

FIGURE 5: Stability lobes with the proportional gain (k_p) of the front AMB varied: k_d = 0.0016.

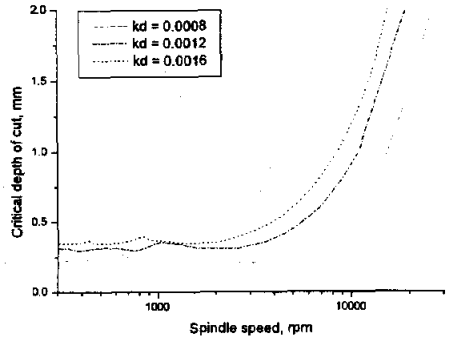

FIGURE 6: Stability lobes with the derivative gain (k_d) of the front AMB varied: k_p = 1.6

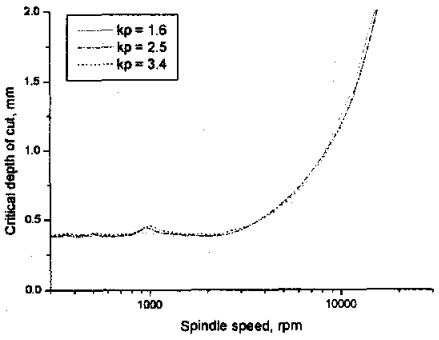

FIGURE 7: Stability lobes with the proportional gain (k_p) of the rear AMB varied: k_d = 0.0032

1. Chatter loop of the milling spindle with AMBs was reviewed and formulated.
2. A new general method for chatter stability analysis was proposed and its effectiveness was verified by comparison with the conventional methods.
3. Recommended guide-lines for selecting the control gains of the AMBs for high speed chatter-free cutting are:
   - The chatter vibrations are not sensitive to the control gains of the rear AMB.
   - The proportional gain of the front AMB may be decreased up to the lower value in the stable region,

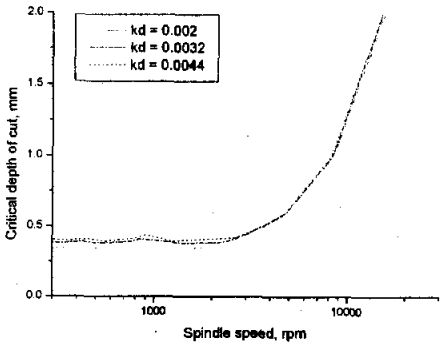

FIGURE 8: Stability lobes with the derivative gain (k_d) of the rear AMB varied: $k_p = 1.6$

but the derivative gain of the front AMB should be large enough to avoid the chatter vibration of the milling spindle for good surface finish in milling.

REFERENCES

1. Tonshoff, H. K., Wobker, H. G. and Blawit, C., High speed cutting of grey cast iron, Fourth International Symposium on Magnetic Bearings, ETH Zurich, Switzerland, August, 1994.
2. Taniguchi, M., Ueyama, H., Nakamori, M. and Morita, N., Cutting performance of digital controlled milling AMB spindle, Fifth International Symposium on Magnetic Bearings, Kanazawa, Japan, August, 1996
3. Tlusty, J. and Polacek, M., The stability of machine tools against self excited vibrations in machining, International Research in Production Engineering, ASME, pp. 465 – 474, 1963
4. Merritt, H. E., Theory of self - excited machine tool chatter, ASME Journal of Engineering for Industry, Vol. **87**, pp. 447 – 454, 1965
5. Sridhar, R., Hohn, R. E. and Long, G. W., General formulation of the milling process equation, ASME Journal of Engineering for Industry, Vol.**90**, pp. 317 – 324, 1968
6. Lee, A. C. and Liu, C. S., Analysis of chatter vibration in the end milling process, International Journal of Machine Tool Design and Research, Vol. **31**(4), pp. 471 – 479, 1991
7. Altintas, Y. and Budak, E., Analytical prediction of stability lobes, Annals of the CIRP, Vol. **44**, pp. 357-362, 1995
8. Franklin, G. F., Powel, J. D. and Naeini, A. E., Feedback control of dynamic systems, Addison-Wesley, 1994
9. Tlusty, J. and Ismail, F., Basic nonlinearity in maching chatter, Annals of the CIRP, Vol. **30**, pp. 21–25, 1981
10. Lee, C. W., Vibration analysis of rotors. ,Kluwer Academic Publishers, 1993
11. Geoffrey, B., Fundamentals of metal machining and machine tools., Scripta Book Co., Washington, D.C., 1975

APPENDIX A

$$M_c = \frac{1}{(l_{s1}+l_{s2})^2}\begin{bmatrix} ml_{s2}^2 + I_t & ml_{s1}l_{s2} - I_t & 0 & 0 \\ ml_{s2}l_{s1} - I_t & ml_{s1}^2 + I_t & 0 & 0 \\ 0 & 0 & ml_{s2}^2 + I_t & ml_{s1}l_{s2} - I_t \\ 0 & 0 & ml_{s1}l_{s2} - I_t & ml_{s1}^2 + I_t \end{bmatrix}$$

$$G_c = \frac{1}{(l_{s1}+l_{s2})^2}\begin{bmatrix} 0 & 0 & I_p\Omega & -I_p\Omega \\ 0 & 0 & -I_p\Omega & I_p\Omega \\ -I_p\Omega & I_p\Omega & 0 & 0 \\ I_p\Omega & -I_p\Omega & 0 & 0 \end{bmatrix}$$

$$B_F = \frac{1}{(l_{s1}+l_{s2})}\begin{bmatrix} l_{s2}+l_c & 0 \\ 0 & l_{s1}-l_c \\ l_{s2}+l_c & 0 \\ 0 & l_{s1}-l_c \end{bmatrix}$$

$$K_{cy} = diag\left[-k_{y1}, -k_{y2}, -k_{z1}, -k_{z2}\right] \quad B_c = diag\left[k_{iy1}, k_{iy2}, k_{iz1}, k_{iz2}\right]$$

$$K_p = diag\left[k_{py1}, k_{py2}, k_{pz1}, k_{pz2}\right] \quad K_d = diag\left[k_{dy1}, k_{dy2}, k_{dz1}, k_{dz2}\right]$$

APPENDIX B

$$A = \begin{bmatrix} 0 & 0 & 0 & 0 & 0 & E_6 \\ 0 & 0 & 0 & 0 & E_6 & E_5 \\ 0 & 0 & 0 & E_6 & E_5 & E_4 \\ 0 & 0 & E_6 & E_5 & E_4 & E_3 \\ 0 & E_6 & E_5 & E_4 & E_3 & E_2 \\ E_6 & E_5 & E_4 & E_3 & E_2 & E_1 \end{bmatrix} \quad B = \begin{bmatrix} 0 & 0 & 0 & 0 & E_6 & 0 \\ 0 & 0 & 0 & E_6 & E_5 & 0 \\ 0 & 0 & E_6 & E_5 & E_4 & 0 \\ 0 & E_6 & E_5 & E_4 & E_3 & 0 \\ E_6 & E_5 & E_4 & E_3 & E_2 & 0 \\ 0 & 0 & 0 & 0 & 0 & -E_0 \end{bmatrix}$$

where

$$E_6 = \alpha_1 M_c \,, \quad E_5 = \alpha_2 M_c + \alpha_1 G_c \,, \; E_4 = \alpha_3 M_c + \alpha_2 G_c + \alpha_1 K_{cy}$$

$$E_3 = \alpha_4 M_c + \alpha_3 G_c + \alpha_2 K_{cy} + \alpha_5 B_c (K_p K_d + K_d) + \alpha_6 B_F A_0 T_c$$

$$E_2 = M_c + \alpha_4 G_c + \alpha_3 K_{cy} + \alpha_7 B_c (K_p K_d + K_d) + \alpha_5 B_c K_p + \alpha_8 B_F A_0 T_c$$

$$E_1 = G_c + \alpha_4 K_{cy} + \alpha_9 B_c (K_p K_d + K_d) + \alpha_7 B_c K_p + \alpha_{10} B_F A_0 T_c$$

$$E_0 = \alpha_9 B_c K_p + K_{cy}$$

$$\alpha_1 = \frac{1}{12}\tau_a\tau_c\left(\frac{T}{N}\right)^2, \quad \alpha_2 = \frac{1}{2}\tau_a\tau_c\left(\frac{T}{N}\right) + \frac{1}{12}(\tau_a+\tau_c)\left(\frac{T}{N}\right)^2$$

$$\alpha_3 = \tau_a\tau_c + \frac{1}{2}(\tau_a+\tau_c)\left(\frac{T}{N}\right) + \frac{1}{12}\left(\frac{T}{N}\right)^2$$

$$\alpha_4 = \tau_a + \tau_c + \frac{1}{2}\left(\frac{T}{N}\right), \quad \alpha_5 = \frac{1}{12}k_{amp}k_s\left(\frac{T}{N}\right)^2$$

$$\alpha_6 = \frac{1}{2}bK_t\tau_a\tau_c\left(\frac{T}{N}\right), \quad \alpha_7 = \frac{1}{2}k_{amp}k_s\left(\frac{T}{N}\right)$$

$$\alpha_8 = \frac{1}{2}bK_t(\tau_a+\tau_c)\left(\frac{T}{N}\right), \; \alpha_9 = k_{amp}k_s, \; \alpha_{10} = \frac{1}{2}bK_t\left(\frac{T}{N}\right)$$

Here τ_a and τ_c are the 1st order power amplifier and low pass filter time constants of the PD controller; k_{amp} and k_s are the constant power amplifier and the sensor gains.